

# On the study of local stress rearrangements during quasistatic plastic shear of a model glass: do local stress components contain enough information?

Michel Tsamados<sup>1</sup>, Anne Tanguy<sup>1</sup>, Fabien Léonforte<sup>2</sup>, Jean-Louis Barrat<sup>1</sup>

<sup>1</sup> Université de Lyon; Univ. Lyon I, Laboratoire de Physique de la Matière Condensée et Nanostructures; CNRS, UMR 5586, 69622 Villeurbanne, France

<sup>2</sup> INSA Lyon, MATEIS, 69621 Villeurbanne, France

Received: date / Revised version: date

**Abstract.** We present a numerical study of the mechanical response of a 2D Lennard-Jones amorphous solid under steady quasistatic and athermal shear. We focus here on the evolution of local stress components. While the local stress is usually taken as an order parameter in the description of the rheological behaviour of complex fluids, and for plasticity in glasses, we show here that the knowledge of local stresses is not sufficient for a complete description of the plastic behaviour of our system. The distribution of local stresses can be approximately described as resulting from the sum of localized quadrupolar events with an exponential distribution of amplitudes. However, we show that the position of the center of the quadrupoles is not related to any special evolution of the local stress, but must be described by another variable.

**PACS.** PACS-key describing text of that key – PACS-key describing text of that key

## 1 Introduction

While the mechanical plastic response of crystalline solids is now well described in terms of elementary defects called dislocations, the plastic response of amorphous solids is not so well understood, and has been the object of numerous studies in the past two decades. Most theoretical works [1, 2, 3, 4, 5, 6, 7, 8, 9, 10, 11, 12, 13, 14, 15, 16, 17, 18, 19], on the forced dynamics of glassy materials assume that the irreversible evolution of glasses occurs through localized, irreversible events. Such events have been well identified in simulations of 2D models [1] and are referred to as shear transformation zones (STZ) or quadrupolar events [18, 19, 20, 21] and are somewhat similar to T1 events in the rheology of 2D foams [22].

These localized and dissipative events should correspond to the “soft mode” of the material [18, 19, 23, 24]), which is the first mode to become unstable, when the system reaches a limit of mechanical instability. However, the local and intermittent nature of the plastic events complicates the identifica-

tion of the corresponding order and control parameters. Experimental studies on disordered materials, far below the glass transition temperature [22, 25, 26, 27, 28, 29, 30, 31, 32], support the existence of a collective behaviour of localized rearrangements leading to a strongly heterogeneous mechanical response as shown in the existence of shear bands in the macroscopic plasticity of such systems. It has also been shown experimentally [32, 33, 34] as well as numerically [1, 18, 21, 35, 36, 37] while studying the stress-strain response of amorphous materials that, in the so called plastic regime, these events lead to an intermittent release of the macroscopic stress in the material. The understanding of the role played by local stresses in the macroscopic mechanical behaviour of such systems is thus very important. Since these systems are known to have a wide distribution of local stresses, mesoscopic models [7, 10, 11, 38] propose precisely to relate the existence of shear bands to the local rearrangements due to local thresholds and activated dynamics in the local stress itself. In these models, the collective effects would thus be due to long-

range elastic couplings in solid systems, and the irreversible behaviour would be associated with local stress thresholds, and avalanche dynamics.

In the present paper, we provide an extensive study of the local stress dynamics in the quasi-static plastic response of a model glass at very low temperature, and in the plastic flow regime. The system we have studied is a 2D Lennard-Jones glass, already studied previously for understanding the heterogeneous mechanical response in the elastic regime, far below plastic flow [39,40,41,42,21]. In the first part of this paper, we discuss the evolution of the local stresses (local pressure, deviatoric stress) in the plastic flow regime, within the framework of dynamical heterogeneities [43]. We show the existence of a finite size of cooperativity appearing in the plastic flow regime, even in the limit of zero temperature and quasi-static shear. In the second part of this paper, we provide a detailed analysis of the full statistical properties of the stress components (pressure, shear stress). We show that the temporal correlations shown in the local particle rearrangements for small imposed strain [21,19] are absent in the average evolution of local stress components. We then show in the third part of this paper, that the statistical evolution of stress components can be described as resulting simply from a sum of localized quadrupolar rearrangements. This description allows us to propose a simple equation of evolution for the local stress depending unfortunately on a local yet unknown criterion for instability. In the last part, we show that this local criterion for instability is not related to any stress threshold but could be related to a different variable, such as the local stress increments.

## 2 Dynamical heterogeneity

### 2.1 Two points correlation function

The system we study numerically has already been described extensively in previous articles [40,41,42,21]). It is a 2D glass obtained by quenching very quickly a liquid sample obtained by molecular dynamics simulations, and made of polydisperse particles interacting through a Lennard-Jones potential. In the following, all quantities will be expressed in Lennard-Jones units ( $u_{LJ}$ ), that is an energy  $\epsilon_{LJ} = 1$  ( $\approx 0.1eV$ ), a distance  $\sigma_{LJ} = 1$  ( $\approx 2\text{\AA}$ ) and mass  $m = 1$  ( $\approx 10g.mol^{-1}$ ). The number of particles per unit surface is  $\rho = 0.925$ , corresponding to very small pressure  $P \approx 0.2$  at rest. The system is made of at least  $N = 10000$  particles, corresponding to a square with a linear size of 104 interatomic

distances. Larger systems have also been considered, especially in this paper a system of  $N = 23125$  particles, corresponding to a rectangular box of size  $50 \times 500$ . These large system sizes are necessary in order to avoid strong finite size effects. The quenching starts from the liquid state, at a temperature  $T = 2$ . Then the system is relaxed using MD to a given temperature of  $1 - 0.5 - 0.1 - 0.05 - 0.01 - 0.005 - 0.001$ , where it is aged during 1000 unit times. The final step is a relaxation at zero temperature, using the Conjugate Gradient Method in order to get an instantaneous minimization of the potential energy. The system being at zero temperature, it is sheared quasi-statically, by imposing successive steps of global shear strain  $\delta\epsilon = 5.10^{-5}$  on the walls. After each step, the system is relaxed into its nearest equilibrium position, thus ensuring that the applied mechanical deformation is quasi-static. The local stress components are computed on each particle  $i$  by using the usual Irving-Kirkwood formula ([44])

$$\sigma_{\alpha\beta,i} \equiv -1/V_i \cdot \sum_j t_{ij} d_{\alpha} \cdot d_{\beta} \cdot r_{ij}$$

$V_i$  being the volume of the Voronoi cell,  $t_{ij}$  the amplitude of the interacting force between particles  $i$  and  $j$ ,  $r_{ij}$  the distance between particles and  $\vec{d}$  the unit vector of the bond. The macroscopic stresses are obtained by averaging the local stress components over the whole system, or alternatively by measuring the force per unit length acting on the walls along appropriate directions. In Fig.1, we show the (averaged) macroscopic shear stress as a function of the total strain applied to the system. The global shear stress has an intermittent behaviour, with an alternance of small and large jumps, giving rise to negative slopes that are the signature of dissipative events. Note that the distribution (figure 2) of these incremental stresses is peaked around the value given by the elastic response with an elastic shear modulus  $\mu \approx 11.7$  ([40]) and shows around this value softer, as well as more rigid, steps.

In order to characterize the evolution of the stress in the flowing regime, we first compute the two points correlation function of the local stress components acting on each particle inside the sample. The correlation function is ‘‘Lagrangian’’ in the sense that the stress is followed on a given particle as the system is sheared. In the plastic flow regime, we expect the system reaches a stationary steady state with time-translational invariant (TTI) observables and correlations. Note that in quasistatic simulation, time does not appear explicitly and must be interpreted in the following as the number of steps  $n$  of elementary shear strain  $\delta\epsilon$  applied to the system.

The total imposed strain is thus  $\epsilon = n.\delta\epsilon$ . In order to study the stress fluctuations correlation function, we introduce the notation  $\rho(\vec{r}, n) \equiv \sigma(\vec{r}, n) - \overline{\sigma(n)}$  where  $\overline{A}$  denotes a spatial average and  $\vec{r}$  is the position of the particle;  $\sigma$  is a component of the stress tensor, namely  $\sigma \equiv \sigma_{dev}$  where  $\sigma_{dev} \equiv \sigma_1 - \sigma_2$ ,  $\sigma_1$  and  $\sigma_2$  being the eigenvalues of the local 2x2 stress tensor; or  $\sigma \equiv \sigma_p$  where  $\sigma_p = -(\sigma_1 + \sigma_2)/2$  is the local pressure; or  $\sigma \equiv \sigma_{xy}$  is the local shear stress. The two-time autocorrelation function of the stress fluctuations writes

$$C(\Delta n, n) = \overline{\rho(\vec{r}, n + \Delta n)\rho(\vec{r}, n)}, \quad (1)$$

and

$$\begin{aligned} C(\Delta n) &= \langle C(\Delta n, n) \rangle \\ &= \overline{\langle \rho(\vec{r}, n + \Delta n)\rho(\vec{r}, n) \rangle} \\ &\approx C(\Delta n, n), \end{aligned} \quad (2)$$

where the last equality assumes TTI.

Numerically we have computed the stress components (as mentioned before from the Irving-Kirkwood definition, denoted by  $\sigma_i(n)$ ) on each particle of the system. The discrete version of the above equation writes

$$C(\Delta n) = \frac{1}{N} \langle \sum_i \rho_i(n + \Delta n)\rho_i(n) \rangle. \quad (3)$$

where  $\rho_i(n) = \sigma_i(n) - \overline{\sigma(n)}$ . We have computed this quantity in the plastic flow regime (i.e. for external shear deformation  $\epsilon$  greater than 1.5%), where the average total stress saturates and fluctuates around a given average value  $\sigma_Y$ . We checked that the correlations are invariant under time translation and in Fig. 3 we plot the autocorrelation function for the shear component of the stress, on a lin-log scale and normalized to 1 for  $\Delta n = 0$ . The behaviour can be decomposed into two successive relaxations. It starts with a first exponential decay at small deformation with a characteristic strain of 3.1%, this decrease to a plateau is analogous to the  $\beta$  - relaxation in supercooled liquids, and is followed by an apparent stretched exponential decay. A similar Kohlrausch-Williams-Watts [45, 46] is usually observed in supercooled liquids and ageing glassy systems, with a correlation that evolves as  $C(t) = A \exp(-(t/\tau)^\beta)$  with  $\beta \leq 1$ . This behaviour is approximately recovered in our systems at large deformations (see inset of Fig. 3), with the exponent  $\beta = 0.7$ . For small strains, the relaxation is strictly exponential. Note that the large strains stretched exponential decay could also be seen as the best fit for an intermediate regime between two

successive exponential decays (see the fit by an exponential decay with characteristic strain  $\epsilon \approx 10\%$  at very large strains in Fig. 3). In any case, the presence of dissipative events leads to the relaxation of local stress at large deformations, above a few percents of strain.

## 2.2 Four points correlation function or cooperativity number

In the recent years, the quest for a dynamical cooperativity length associated with the slowing down of the dynamics of supercooled liquids [43, 47, 48] has led to the development of new statistical tools to characterize such “dynamical heterogeneities”. In our previous paper [21] we showed that the motion of the particles in our system under shear is highly non trivial. It shows a background of heterogeneous motion even in the elastic regime at very low temperature; for larger applied strains, in the plastic regime, it shows zones of very high mobility located in the vicinity of elementary shear bands and of localized quadrupolar events, and similarly zones of low mobility far from these irreversible events (the local displacement field can vary by many orders of magnitudes). This type of behaviour in the mechanical response of glass, even at zero temperature, can be seen as some kind of dynamical heterogeneity (while the “dynamics” here is overdamped) and it is of great interest to quantify a cooperativity degree or a cooperative length scale. To do so, Berthier et al. [43] have proposed to look at the so called  $\chi_4$  four point correlation function. An other possible observable is the cooperativity number introduced by Doliwa and Heuer [47], that estimates the spatial fluctuations of the two-point correlation function introduced previously. Following reference [47] the definition we use here is

$$N_{coop} \equiv \frac{Var[\sum X_i]}{\sum Var[X_i]} = \frac{\langle \{\sum_i X_i - \langle \sum_i X_i \rangle\}^2 \rangle}{\sum_i \langle \{X_i^2 - \langle X_i \rangle^2\} \rangle}, \quad (4)$$

where  $X_i(t', t) = (\sigma_i(t+t') - \overline{\sigma_i(t+t')})(\sigma_i(t) - \overline{\sigma_i(t)})$  is a dynamical quantity associated with every particle  $i$ , and computed on various components  $\sigma$  of the stress tensor. In Eq.(4), one shows easily that in the case of totally uncorrelated variables  $X_i$  ( $\langle X_i X_j \rangle = 0$ ), one gets  $N_{coop} = 1$ , but in the opposite if the correlation is complete ( $X_i = X_j$ ) one gets  $N_{coop} = N$ . Finally in the case of  $L$  independent groups each comprising  $M$  identical variables and of zero mean ( $N = LM$ ) one gets

$$\begin{aligned}
N_{coop} &= 1 + \frac{\sum_{i \neq j} \langle X_i X_j \rangle}{\sum \langle X_i^2 \rangle} \\
&= 1 + \frac{1}{\sum \langle X_i^2 \rangle} \sum_{i=1}^N \sum_{j=1}^{M-1} \langle X_i^2 \rangle = M. \quad (5)
\end{aligned}$$

The cooperativity number is obtained by averaging over the origins  $t$  and remains a function of time  $t'$  ( $N_{coop}(t')$ ). Note that this function does not contain any useful information on the heterogeneous motion in the linear elastic regime, since in this case, the amplitude of the stress on each particle increases linearly with time. The cooperativity number is thus constant in this regime. A maximum can be reached only in the non-linear regime, like in the plastic flow regime here, or when thermal activation starts playing a role. In Fig. 4 we have plotted this function computed on all particles located at a distance of a few (typically 10) particle diameters from the boundaries, and for different components of the stress tensor. All the stress components have approximately the same contribution to the cooperativity number, with a maximum of a few tens at an imposed strain of a few percents ( $\approx 4\%$ ). As described before, the maximum is a measure of the maximum number of particles on which the local stress evolves in a correlated manner. In our case, it corresponds to an ensemble of  $6 \times 6$  to  $7 \times 7$  particles where the stress components evolve in a cooperative way. The strain at which this maximum is reached is about 4 percents, that is beyond the plastic threshold, and close to the characteristic strain obtained from the two points correlation function  $C$ . This picture corresponds to the description of localized plastic events, that we have made already in a preceding paper [21]. In the elastic regime (as in elastic branches present in the plastic flow plateau [21]), the cooperative evolution of stress can be more important, but does not contribute significantly to the cooperativity number.

Fig. 4 shows that there are strong boundary effects measurable on this quantity. Indeed, the cooperativity number is much higher in the vicinity of the walls ( $\approx 100$ ) corresponding to a layer of one particle diameter along the entire system size ( $L_x = 104$ ). Finally, note that this maximum cooperativity number is finite in the quasi-static limit studied here, suggesting a saturation at very low shear rate.

### 3 Statistical analysis of the local shear stress

In the previous section we have studied the average evolution of the stress components by looking at averaged quantities like the number of cooperativity, or the two-point correlation function. We will now examine in details the full histogram of stress changes. The results are shown here for the shear stress component, but we have checked that all the following results are also valid for other components (pressure and deviatoric stress). In figure 5 we show the typical evolution of the shear stress component on a given particle up to a total strain of 25%<sup>1</sup>. The variations of stresses are larger than expected if they would be Brownian. In order to analyze this evolution, we have plotted in figure 6 the distribution  $P(\Delta\sigma_{xy}, \Delta n)$  of the shear stress increments

$$\begin{aligned}
\Delta\sigma_{xy}(\Delta n, n) &\equiv (\sigma_{xy}(n + \Delta n) - \bar{\sigma}_{xy}(n + \Delta n)) \\
&\quad - (\sigma_{xy}(n) - \bar{\sigma}_{xy}(n)) \quad (6)
\end{aligned}$$

for various numbers  $\Delta n$  of incremental shear steps ( $\Delta n = 1, 2, 4, 8, 16\dots$ ), averaged over the origins  $n$  and over the entire system. The distributions  $P(\Delta\sigma_{xy}, \Delta n)$  are all symmetric, with zero mean. For  $\Delta n \rightarrow \infty$  one recovers a gaussian distribution, which is consistent with the central limit theorem. However, at small imposed strains, these distributions are not gaussian as would be the case for a Brownian evolution. A finer analysis of the distribution of the elementary increments  $P(\Delta\sigma_{xy}, \Delta n = 1)$  (see fig 6b and c) shows three zones. At small incremental stress jumps  $\Delta\sigma_{xy}$ , we can see a plateau of approximately constant probability, whose width evolves inversely proportional to the volume  $V$  of the sample, followed by an apparent power-law decay, in a zone of approximately three decades for  $100/V \leq \Delta\sigma_{xy} \leq 10$  where  $P(\Delta\sigma_{xy}, \Delta n = 1) \propto 1/\Delta\sigma_{xy}^{\alpha+1}$ , and concluded by an exponential cut-off independent on the system size (characteristic shear stress  $\Delta\sigma_{xy} \approx 1.4$ ). This upper cut-off allows for a finite variance of the local stress evolution. In the absence of any temporal correlations, the entire process can thus be described by the central limit theorem, with a scale invariant distribution on a finite interval. In this intermediate stress range, the probability density function (hereafter, pdf)  $P(\Delta\sigma_{xy}, \Delta n)$  is well reproduced by the scale invariant relation

<sup>1</sup> In a previous paper we have analyzed in a similar way the motion of a particle in the system under shear (see Ref. [21])

$$\begin{aligned}
P(\Delta\sigma_{xy}, \Delta n) &= \Delta n^{-H} f\left(\frac{|\Delta\sigma_{xy}|}{\Delta n^H}\right) \\
&\text{or} \\
P(\Delta\sigma_{xy}, \Delta\epsilon) &= \Delta\epsilon^{-H} f\left(\frac{|\Delta\sigma_{xy}|}{\Delta\epsilon^H}\right)
\end{aligned} \quad (7)$$

with

$$f(u) \propto \begin{cases} u^0, & \text{for } u \ll 1 \\ u^{-\alpha-1}, & \text{for } 1 \ll u \ll cste. \Delta n^{-H} \end{cases} \quad (8)$$

In the intermediate stress range, the process can thus be considered as self-similar. Fig 7(a) illustrates this scaling with a good superposition of the distributions for  $\alpha = 0.7$  and  $H \simeq \frac{1}{\alpha}$  (only for not too large  $\Delta n$  since for very large  $\Delta n$  the upper cut-off discussed before contributes significantly to the resulting distribution). The exponent  $\alpha$  describes the algebraic (slow) asymptotical decay of the distribution of the incremental jumps  $P(\Delta\sigma = s, \Delta n = 1) \propto s^{-\alpha-1}$  (as shown in fig 6(a)). The exponent  $H$  is related to the evolution of the stress jumps as a function of the applied shear strain  $\Delta n$ . It characterizes the  $\Delta n$ -dependence of the crossover between a regime of approximately uniform probability (for  $|\Delta\sigma| \ll \Delta n^H$ ) and the power law regime (for  $|\Delta\sigma| \gg \Delta n^H$ ). The coefficient  $H$  also accounts for possible temporal statistical correlation between jumps. As stated in Taqqu et al. [49] the only non degenerate  $\alpha$ -stable self similar processes with stationary increments that verify  $H = \frac{1}{\alpha}$  and where  $0 < \alpha < 1$  are the  $\alpha$ -stable Lévy motions. As described above, the evolution of the shear stress is thus of Lévy flight type, but only in the intermediate stress (and applied strain) range. The Lévy flight evolution implies by definition, first that there is no temporal correlation between local stress jumps during the shear of the sample, second that the variance of elementary changes is infinite (as long as the exponential cut-off is neglected)<sup>2</sup>. These results can be compared with the study of the pdf  $P(\Delta y, \Delta n = 1)$  of the positional jumps in the transverse direction, that showed in contrary that these jumps were correlated in time for small imposed deformation [21].

According to the above, a plausible equation that would describe the evolution within a Lévy

flight process for the stress component  $\sigma$ , averaged over the whole system, is

$$\frac{d(\sigma(i, \epsilon) - \bar{\sigma}(\epsilon))}{d\epsilon} = \eta(i, \epsilon) \quad (9)$$

where  $\eta(i, \epsilon)$  is a stochastic process whose spatial average  $\bar{\eta}(\epsilon)$  is the process that is entirely characterized above (ie by the distribution of the elementary increment and by the absence of correlation between successive increments), and  $\epsilon$  is the *external* imposed shear strain. For small imposed shear strain, it can be mentioned that such an equation with a noise corresponding to a Lévy motion cannot be reinterpreted in terms of the usual Fokker-Planck equation as the moments of the shear stress  $\sigma$  are non vanishing for all orders. However, for large strain intervals  $\Delta\epsilon$ , the stochastic process becomes gaussian, due to the existence of the upper cut-off in the distribution of  $\bar{\eta}$ .

We will now propose a microscopic origin for the elementary process  $\eta$ , by comparing it with a spatial redistribution of quadrupolar stress.

But before, it can be interesting (as in Ref. [19, 20]) to identify the contribution to the distribution  $P(\Delta\sigma, \Delta n)$  of events with a release of the macroscopic stress (plastic events with  $\Delta\sigma_{macro} < 0$ ). This is shown in figure 7(b). We see here that for large imposed strains ( $\Delta n > 64$  it means  $\Delta\epsilon > 0.32\%$  - smaller than the observed plastic threshold) the contribution to the distribution is mainly due to plastic events meaning that the weight of elastic events is negligible in this range of applied strain. This corresponds also to the strain interval  $\Delta n$  at which the distribution becomes gaussian with a good approximation (non gaussian parameter less than 1), and where the departure from Lévy motion is of course noticeable. For smaller strains, the contribution of steps with an increase of the macroscopic stress ( $\Delta\sigma_{macro} > 0$ ) influences the distribution mainly for small values of the local stresses. These positive steps are for example responsible for the different power-law decay ( $\propto 1/\Delta\sigma_{xy}^{2.5}$  in place of  $\propto 1/\Delta\sigma_{xy}^{1.7}$ ) in the beginning of the first crossover in the distribution (at the end of the initial plateau). We are unable to explain the precise value of these two exponents. However, we will now propose a model that is able to explain the generic features of this distribution of shear stress increments.

## 4 Minimal model: sum of quadrupoles

As shown in [21], the plastic flow regime consists in a succession of elastic branches and plastic events. We will now focus on the contribution of plastic

<sup>2</sup> In the case of Brownian motion the properties stated above on the pdf and on the process are verified (self similarity,  $\alpha$ -stable process, stationary increments) but with a finite variance ( $\alpha > 2$ ) allowing to a unique value  $H = 1/2$ .

events to the evolution equation of the stress components in the system. We identify here a plastic event by the fact that the associated stress is relaxed macroscopically (corresponding to an evident dissipation of energy shown by a negative slope in the stress-strain response of the system, see Fig.1). Some of them correspond to an isolated quadrupolar redistribution of local stresses around a well identified center inside the sample; other plastic events consists in an alignment of rotational structures in the particle displacements giving rise to elementary shear bands going through the system [21]. The two kinds of events coexist in the plastic flow regime, and the transition from one kind of plastic event to another is still matter of debate [19,34,50,51]. However, the isolated quadrupolar event is more frequent than the elementary shear band. In the linear initial regime for example, only the isolated quadrupolar events take place, while there are periods with only quadrupolar events in the plastic flow regime as well.

In the following, we take the quadrupolar isolated event as the elementary building block for explaining the plastic deformation of the material, and we propose a simple model that describes the plastic deformation (as shown in the redistribution of stresses) as a sum of uncorrelated quadrupoles of random amplitude  $A$ .

We first identify the distribution  $P(A)$  in our system. As shown by Picard et al. [52], a quadrupolar event involves in 2D a long-range redistribution of stresses, due to a local pure shear. The corresponding stress change is of the form.

$$\Delta\sigma_{xy}(r, \theta) \equiv \begin{cases} \frac{A r_0^2}{r^2}, & \text{if } r_0 \leq r \leq r_{max} \\ A, & \text{if } 0 \leq r \leq r_0 \end{cases} \quad (10)$$

where  $r_0$  and  $r_{max}$  are respectively the typical size of the quadrupole and the size of the system,  $A$  is the amplitude of the quadrupoles, and  $\Delta\sigma_{xy}$  denotes the incremental shear stress. We have neglected in this expression the quadrupolar angular dependence of the stress field and only considered its  $\frac{1}{r^2}$  spatial decay<sup>3</sup>. The distribution of  $P(A)$  is measured in our data (see figure 8). It corresponds to the incremental stress at the center of the quadrupole, that is at the place where the displacement is maximum. The best fit is exponential, with  $P(A) = \frac{1}{2\sigma_A} \cdot \exp(-\frac{|A|}{\sigma_A})$  and  $\sigma_A = 2$  appears to be the characteristic amplitude of the quadrupolar

<sup>3</sup> The angular dependence will mainly contribute by a scaling factor, and affect the weight of small  $\Delta\sigma$  in a logarithmic way in the final result. See M.Tsamados et al. *preprint* (2007) for a detailed calculation.

event. It is independent on the system size, unlike the distribution of macroscopic stress release that is  $\propto 1/V$  (figure 2), and is symmetric.

Using the exponential distribution  $P(A)$  shown above, we can now reproduce the distribution  $P(\Delta\sigma = s, \Delta n = 1)$  of the incremental shear stress  $\Delta\sigma_{xy}$  averaged over the whole system. According to the previous analysis (see part III), the distribution for  $\Delta n > 1$  should then be reproduced by successive convolutions, assuming the absence of temporal correlations. Neglecting the angular dependence of  $\Delta\sigma_{xy}$  as in Eq. 10, we show that, for a given amplitude  $A$ , there is a simple bijective relation between the shear stress  $\Delta\sigma_{xy}$  and the radial coordinate  $r$ . We can thus write  $P_A(\Delta\sigma_{xy})d\Delta\sigma_{xy} = P(r)dr$ , with  $P(r)dr = 2\pi r/V dr$ . Using Eq.10, we get

$$P_A(\Delta\sigma_{xy}) = \frac{\pi A r_0^2}{V \Delta\sigma^2} \quad (11)$$

with

$$|A| \frac{r_0^2}{r_{max}^2} \leq |\Delta\sigma_{xy}| \leq |A| \quad (12)$$

In the following, we will consider only the case  $A > 0$ , the opposite case giving the symmetric distribution corresponding to  $\Delta\sigma_{xy} < 0$ . Assuming that the successive events contribute independently to the total distribution  $P(\Delta\sigma_{xy})$  (an assumption justified by the fact that this distribution is averaged over the time origins), the average probability of having an incremental stress  $\Delta\sigma_{xy}$  inside the system is thus obtained by summing over all quadrupolar events

$$P(\Delta\sigma_{xy}) = c \int_{\Delta\sigma_{xy}}^{\frac{\Delta\sigma_{xy} r_{max}^2}{r_0^2}} P_A(\Delta\sigma_{xy}) P(A) dA \quad (13)$$

with an additional normalisation factor  $c$  due to the limited range of allowed amplitudes. This gives

$$P(\Delta\sigma_{xy}) = c \frac{\pi r_0^2}{2V} \frac{1}{\Delta\sigma_{xy}^2} ((\sigma_A + \Delta\sigma_{xy}) \exp(-\Delta\sigma_{xy}/\sigma_A) - (\sigma_A + \sigma_{xy} \frac{r_{max}^2}{r_0^2}) \exp(-\Delta\sigma_{xy} \cdot r_{max}^2 / (\sigma_A \cdot r_0^2))) \quad (14)$$

We show here that the upper exponential cut-off is proportional to  $\exp(-\Delta\sigma_{xy}/\sigma_A)$  and that the low  $\Delta\sigma$  behavior<sup>4</sup> is dominated by finite size scaling proportional to  $\exp(-\Delta\sigma_{xy} \cdot r_{max}^2 / (\sigma_A \cdot r_0^2))$ . We have plotted this function in figure 9, and compared it with the result obtained numerically. We find a good agreement with the numerical result,

<sup>4</sup> with a logarithmic divergence if the angular dependence is taken into account see M. Tsamados et al. *preprint* (2007).

for  $\sigma_A = 2$ ,  $r_{max} = L = 100$  and  $r_0 = 4$ . The parameter  $r_0$  is the unique free parameter of the fit since  $r_{max}$  scales like the system size and the fitted value for  $\sigma_A$  corresponds to the value obtained in the measured distribution of  $P(A)$  (see figure 8), thus confirming our simple model. The small value obtained for  $r_0$  shows that the plastic quadrupolar events are localized.

This simple model gives us a physical intuition on the origin of the distribution for the increments  $\bar{\eta}$  observed in the averaged evolution equation 9. Therefore we can now make more precise the evolution equation at a local level as

$$\frac{\partial(\sigma(\vec{r}, \epsilon) - \bar{\sigma}(\epsilon))}{\partial \epsilon} = \int d^3 \vec{r}_Q \frac{A(\epsilon) r_0^2}{\|\vec{r} - \vec{r}_Q(\epsilon)\|^2} \rho(\vec{r}_Q, \epsilon) \quad (15)$$

where  $\vec{r}_Q$  is the position where the quadrupolar event has occurred,  $\|\vec{r} - \vec{r}_Q\| \geq r_0$ , and  $\rho(\vec{r}_Q, \epsilon)$  is the number of plastic event per unit strain and unit volume, taking place at  $\vec{r}_Q$  when the external strain is  $\epsilon$ .

As it appears clearly here, this equation is not complete since  $\vec{r}_Q(\epsilon)$  is unknown. In many models [11, 10] the occurrence of a quadrupolar event at position  $\vec{r}_Q$  is triggered by a local stress threshold. In the following section, we discuss the existence of such a criterion.

## 5 Looking for a local threshold

The center of the quadrupolar plastic rearrangements is identified as the place where the particle displacement is the largest [21]. In order to relate the position of the center of the quadrupoles to local stress criteria, we have compared the distribution of the stress components obtained for the whole system, and the value of the same stress component on the particle in the center of the quadrupole, one step before the quadrupole takes place.

The result for the deviatoric stress  $\sigma_{dev} \equiv \sigma_1 - \sigma_2$  is shown in figure 10(a). The distribution of the deviatoric stress in the whole sample is stationary: it is the same in the beginning (for ex. one step before the first plastic event) and in the end (e.g. one step before the last measured plastic event) of the plastic flow. It is remarkable to see in this figure, that the distribution of the deviatoric stress restricted to the center of the quadrupoles (one step before each plastic event) computed for all the plastic events is very close to the previously discussed stationary distribution obtained over the whole sample, and not only in the center of the

quadrupoles. The position of the center of the quadrupoles appears to be unrelated with any threshold value in the local stress components. The saturation of the macroscopic stress, and the associated well defined yield stress  $\sigma_Y$  in these systems can thus be related only to the alternance of increase and decrease of stress and to its intermittent behavior, rather than to any identified local stress threshold. The existence of an apparent macroscopic yield stress is not related to a local yield stress. Note that criterion based on Tresca or Mohr-Coulomb criterion, involving the most probable relation between deviatoric stress and pressure have also been tested in our numerical systems. It shows a general tendency for the pressure to be affinely related to the deviatoric stress in the plastic flow regime. However, this tendency is shared by all the particles in the system, and not only by the particles at the center of the quadrupoles. It thus appears, like in the case of the deviatoric stresses, that a global Mohr-Coulomb criterion, or equivalently -for 2D systems- a Tresca criterion, is valid in the plastic flow regime, but it does not provide a locally selective criterion for plasticity.

Figure 10(b) shows the same distributions as for the deviatoric stress, but for the incremental deviatoric stresses: it means  $\sigma_{dev}(n+1) - \sigma_{dev}(n)$ . In this case, quenched stresses are not taken into account, and a large incremental stress is generally the signature of a large local deformation. The distribution of incremental stresses is also stationary. The distribution restricted to the center of the quadrupoles is displaced to larger increases in the deviatoric stresses. This point has also been mentioned by Robbins et al. [12] and underlines the role played by incremental stresses in the dissipative dynamics of the systems, in comparison with total stresses that are more or less unchanged. It suggests that the incremental stress  $\Delta\sigma$  can be a more important parameter for plastic purposes than the stress  $\sigma$  itself. However, its distribution is very broad, and a criterion based only on the incremental stresses is not very selective: it does not even exclude the possibility for the center of the quadrupole to take place where the increase of the deviatoric stress is not maximum but minimum...

The question of the existence of a local criterion for plasticity appears thus clearly beyond our detailed numerical study of local stress components, and deserves a further studies.

## 6 Conclusion

We have shown in this paper that the local stress components evolve in a heterogeneous way during

quasi-static plastic deformation. It is related to a finite cooperativity number identifying fluctuating zones whose maximum size is approximately  $6 \times 6$  particle diameters in the plastic flow regime. The strain at which these zones form ( $\approx 4\%$ ) is related to the typical strain at which the memory of the local stress seems to be lost in the 2-point correlation function.

It is thus natural to propose a picture of the heterogeneous stress evolution, as a sum of localized plastic events. We have shown in this paper that the averaged evolution of the full distribution of local stress components can be described by a simple model. Within this model, the evolution of local stress components results from the uncorrelated sum of localized quadrupolar rearrangements. The model allows to recover the 3 regimes shown in the distribution: its  $1/V$  dependence at small stresses, in agreement with a local description of the plastic instability, the cross-over to an apparent power-law decay  $\propto 1/\Delta\sigma^{\alpha+1}$  with  $\alpha$  close to 1 in the intermediate range, and for larger stresses a size-independent upper cut-off directly related in our model to the size-independent distribution of stress rearrangements in the center of the quadrupoles.

However, a complete description of local stress rearrangements is still lacking: for example, the observed exponential nature of the distribution of the amplitudes of stress rearrangements in the center of the elementary quadrupoles - a crucial ingredient of our model - is still not explained, and the position of the center of the quadrupoles should be related to a criterion of instability not identified in this paper. This last question especially deserves further studies, since it appears clearly here that the local stresses are not determinant.

Any attempt to describe local plasticity in terms of local stress rearrangements should thus take into account these numerical results before proposing a complete description of the heterogeneous mechanical response in terms of a single evolution equation.

**Acknowledgments** During the course of this work, we have benefited of discussions from L. Bocquet, M. Robbins, S. Roux, P. Sollich, and D. Vandembroucq. Computational support by IDRIS/France, CINES/France and CEA/France is acknowledged.

## References

1. M.L. Falk, J.S. Langer, *Phys. Rev. E* **57**(6), 7192 (1998)
2. M.L. Falk, J.S. Langer, *Phys. Rev. B* **60**, 7062 (1999)
3. P.M. A. S. Argon, V.V. Bulatov, U. Suter, *J. Rheol.* **39**, 377 (1995)
4. V.V. Bulatov, A.S. Argon, *Modell. Simul. Mater. Sci. Eng.* **2**, 185 (1994)
5. V.V. Bulatov, A.S. Argon, *Modell. Simul. Mater. Sci. Eng.* **2**, 167 (1994)
6. V.V. Bulatov, A.S. Argon, *Modell. Simul. Mater. Sci. Eng.* **2**, 203 (1994)
7. P. Sollich, F. Lequeux, P. Hébraud, M.E. Cates, *Phys. Rev. Lett.* **78**, 2020 (1997)
8. P. Sollich, *Phys. Rev. E* **58**(1), 738 (1998)
9. F. Radjai, S. Roux, *Phys. Rev. Lett.* **89**(6), 064302 (2002)
10. J.C. Baret, D. Vandembroucq, S. Roux, *Phys. Rev. Lett.* **89**(19), 195506 (2002)
11. G. Picard, A. Ajdari, F. Lequeux, L. Bocquet, *Phys. Rev. E* **71**(1), 010501 (2005)
12. J. Rottler, M.O. Robbins, *Phys. Rev. E* **68**(1), 011507 (2003)
13. M. Wyart, S.R. Nagel, T.A. Witten, *Europhys. Lett.* **72**, 486 (2005)
14. M. Wyart, *Annales de physique* **30**, 1 (2005)
15. M.J. Demkowicz, A.S. Argon, *Phys. Rev. B* **72**(24), 245205 (2005)
16. C.E. Maloney, A. Lemaître, *Phys. Rev. Lett.* **93**, 16001 (2004)
17. C.E. Maloney, A. Lemaître, *Phys. Rev. Lett.* **93**, 195501 (2004)
18. C.E. Maloney, A. Lemaître, *Phys. Rev. E* **74**(1), 016118 (2006)
19. A. Lemaître, C. Caroli (2007), arXiv:cond-mat/0705.0823
20. A. Lemaître, C. Caroli (2007), arXiv:cond-mat/0705.3122v1
21. A. Tanguy, F. Leonforte, J.L. Barrat, *Eur. Phys. J. E* **20**, 355 (2006)
22. M. Dennin, *Phys. Rev. E* **70**(4), 041406 (2004)
23. D.L. Malandro, D.J. Lacks, *Phys. Rev. Lett.* **81**, 5576 (1998)
24. D. Lacks, M. Osborne, *Phys. Rev. Lett.* **93**, 255501 (2004)
25. R. Besseling, E.R. Weeks, A.B. Schofield, W.C.K. Poon, *Phys. Rev. L.* **99**(2), 028301 (2007)
26. J. Lauridsen, M. Twardos, M. Dennin, *Phys. Rev. Lett.* **89**(9), 098303 (2002)
27. D.W. Howell, R.P. Behringer, C.T. Veje, *Chaos: An Interdisciplinary Journal of Non-linear Science* **9**, 559 (1999)
28. S. Tewari, D. Schiemann, D.J. Durian, C.M. Knobler, S.A. Langer, A.J. Liu, *Phys. Rev. E* **60**(4), 4385 (1999)
29. T. Majmudar, R. Behringer, *Nature* **435**, 1079 (2005)
30. E. Kolb, J. Cviklinski, J. Lanuza, P. Claudin, E. Clement, *Phys. Rev. E* **69**(3), 031306 (2004)

31. G. Debrégeas, H. Tabuteau, J.M. di Meglio, Phys. Rev. Lett. 87(17), 178305 (2001)
32. A. Kabla, G. Debrégeas, Phys. Rev. Lett. 90(25), 258303 (2003)
33. I. Cantat, O. Pitois., Phys of Fluid. 18, 083302 1 (2006)
34. P. Marmottant, C. Raufaste, F. Graner, preprint (2007)
35. D.J. Durian, Phys. Rev. Lett. 75(26), 4780 (1995)
36. F. Varnik, L. Bocquet, J.L. Barrat, L. Berthier, Phys. Rev. Lett. 90(9), 095702 (2003)
37. J.L. E.Bouchbinder, I. Procaccia, Phys. Rev. E 75, 036108 (2007)
38. P. Hébraud, F. Lequeux, Phys. Rev. Lett. 81, 2934 (1998)
39. J.P. Wittmer, A. Tanguy, J.L. Barrat, L. Lewis, Europhys. Lett. 57, 423 (2002)
40. A. Tanguy, J.P. Wittmer, F. Leonforte, J.L. Barrat, Phys. Rev. B 66(17), 174205 (2002)
41. F. Leonforte, A. Tanguy, J.P. Wittmer, J.L. Barrat, Phys. Rev. B 70(1), 014203 (2004)
42. F. Leonforte, R. Boissière, A. Tanguy, J.P. Wittmer, J.L. Barrat, Phys. Rev. B 72(22), 224206 (2005)
43. C. Toninelli, M. Wyart, G.B. L. Berthier, J.P. Bouchaud, Phys. Rev. E 71(4), 041505 (2005)
44. J.H. Irving, J. G.Kirkwood, J. Chem. Phys. 18, 817 (1950)
45. F. Kohlrausch, Pogg. Ann. Phys. 119, 352 (1863)
46. G. Williams, D.C. Watts, Trans. Faraday Soc. 66, 80 (1970)
47. B. Doliwa, A. Heuer, Phys. Rev. E 61, 6898 (2000)
48. N. Lacevic, F.W. Starr, T.B. Schroder, S.C. Glotzer, J. Chem. Phys. 119(14), 7372 (2003)
49. G. Samorodnitsky, M.S. Taqqu, *Stable Non-Gaussian Random Processes: Stochastic Models with Infinite Variance.* (2000)
50. P. Marmottant, F. Graner, to appear in Eur. Phys. J. E (2007)
51. F. Graner, B. Dollet, C. Raufaste, P. Marmottant, preprint (2007)
52. F.L. G. Picard, A. Ajdari, L. Bocquet, The European Physical Journal E - Soft Matter 15, 371 (2004)

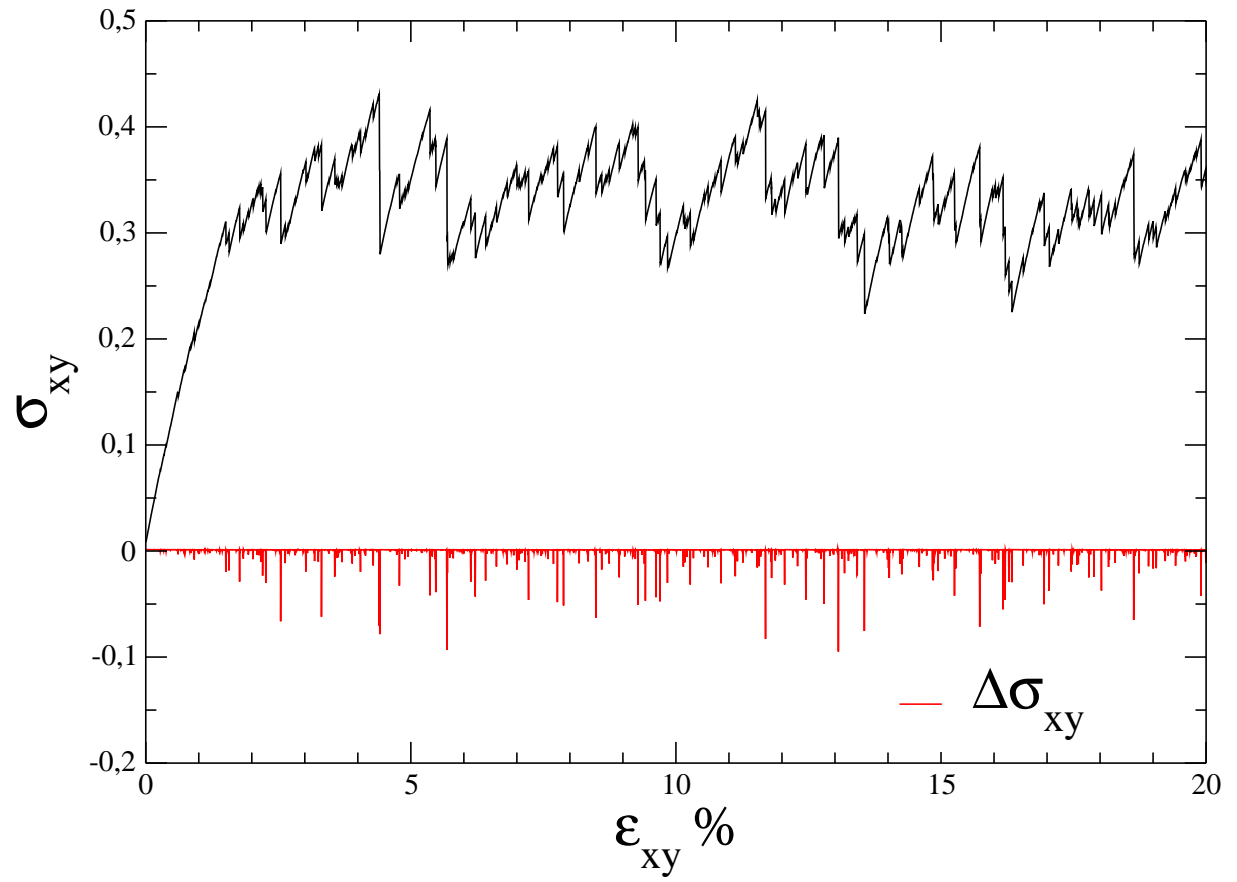
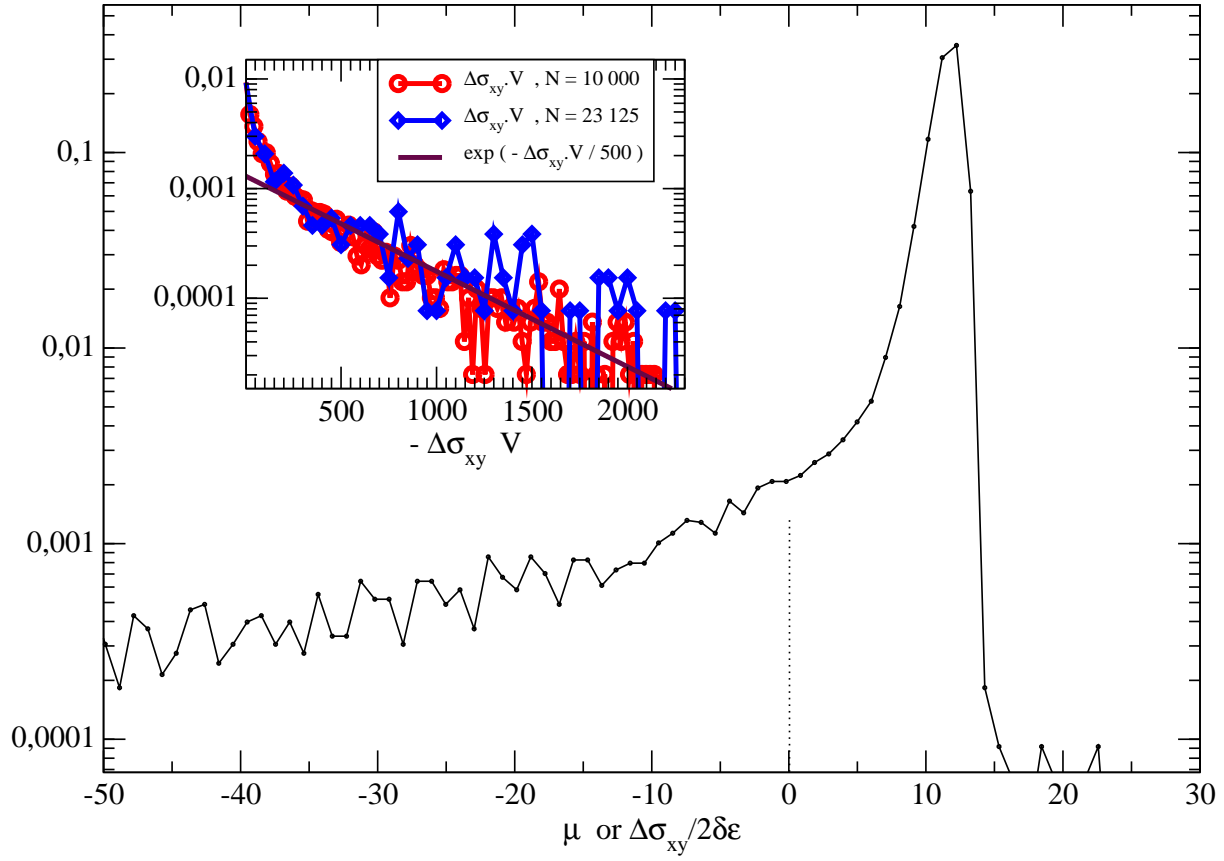
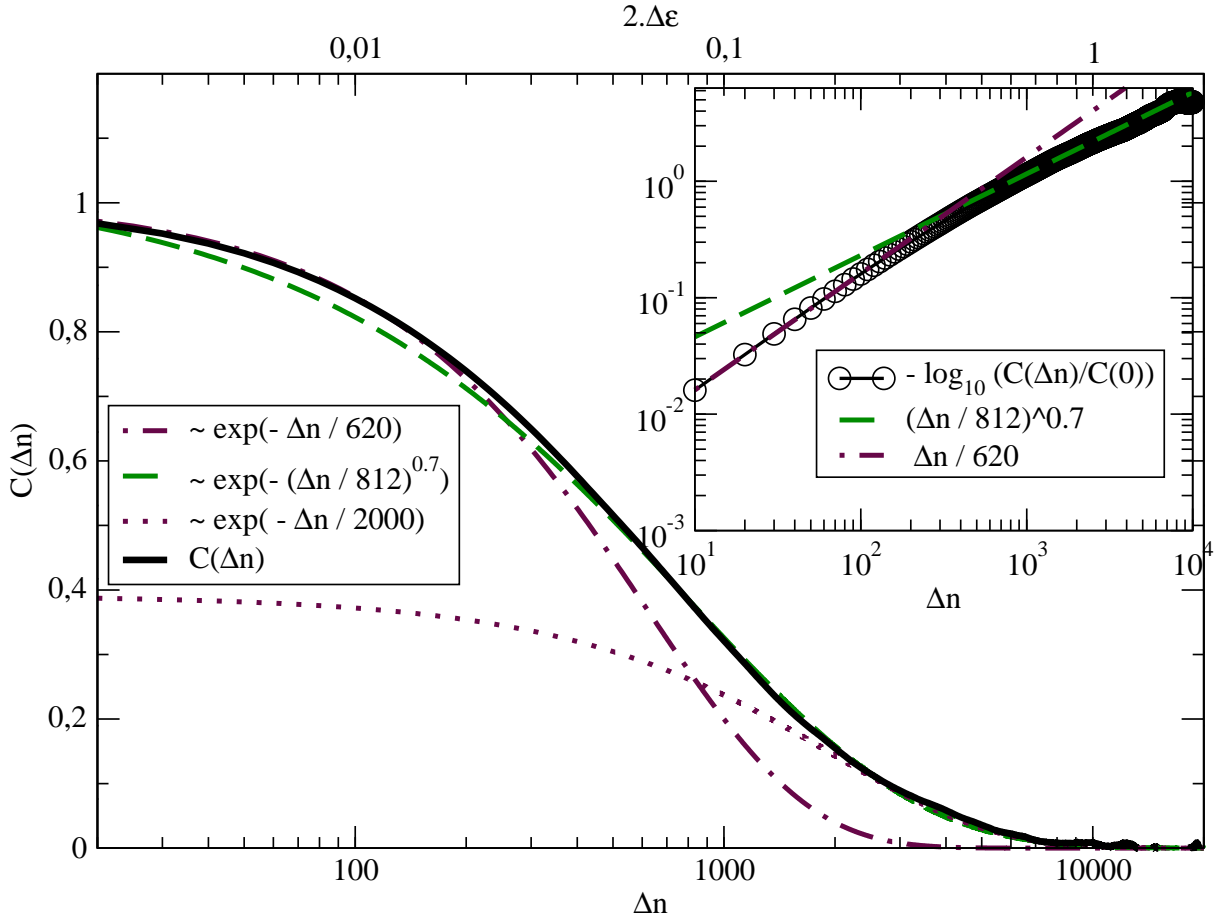


Fig. 1. stress-strain response and incremental shear stress, for one configuration of 10 000 particles.



**Fig. 2.** Histogram of the slope  $\Delta\sigma/\Delta\epsilon$  of the macroscopic shear stress. Inset: Size dependence of the amplitude of negative stress changes  $\Delta\sigma_{xy}$ . The amplitude of stress releases is proportional to the volume of the sample.



**Fig. 3.** Autocorrelation function of the shear stress computed on each particle and averaged over the whole sample, as a function of time (applied shear strain). The nature of the fits is indicated in the legend box. Inset: Logarithm of the Autocorrelation function of the shear stress, in log-log scale, in order to determine the exponent of the corresponding stretched exponential

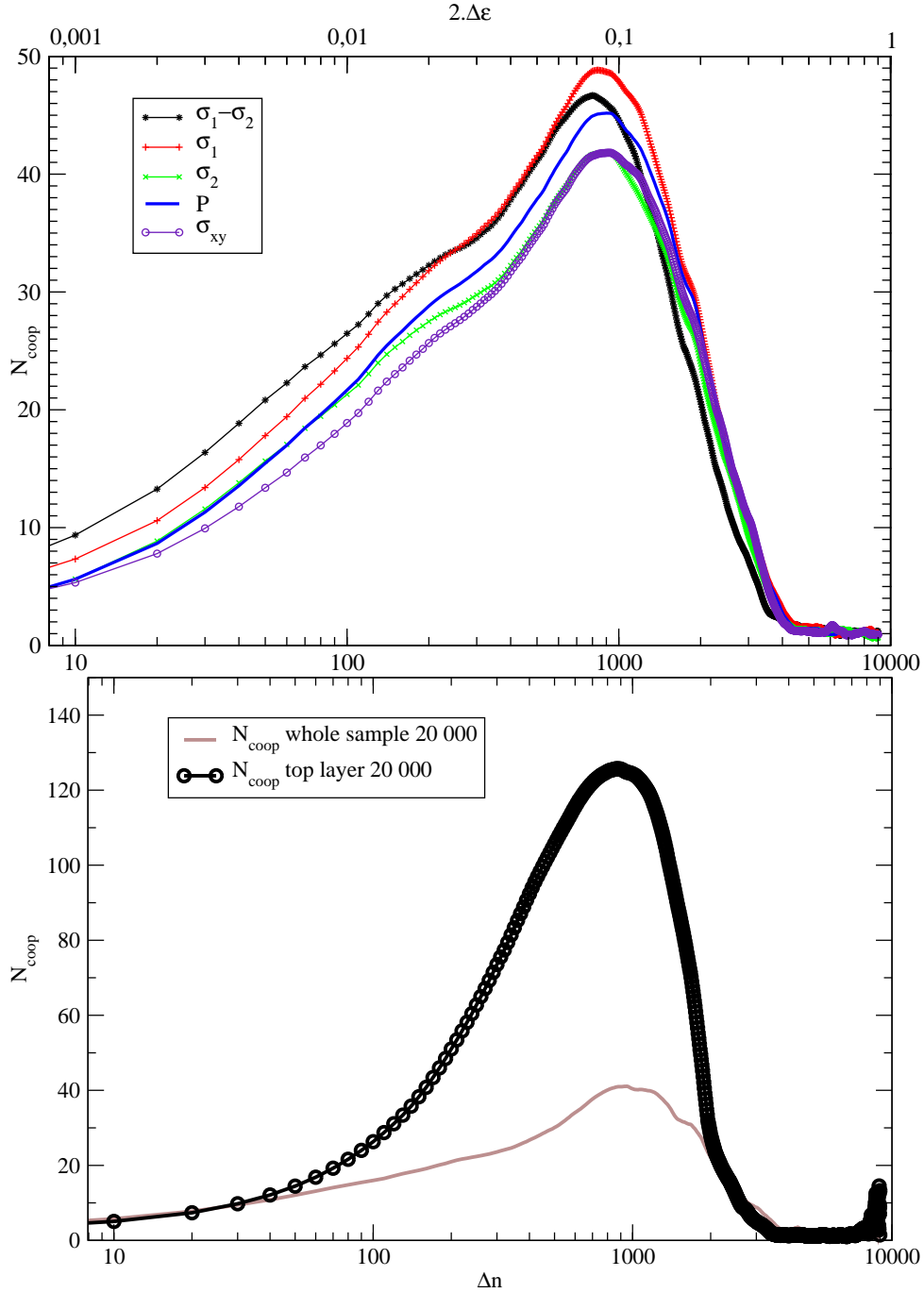


**Fig. 4.** (a) Cooperativity number as a function of time (applied shear strain) for various stress components: local shear stress  $\sigma_{xy}$ , local pressure  $P$ , eigenvalues of the stress tensor  $\sigma_1$  and  $\sigma_2$ , and the deviatoric stress  $\sigma_{dev} = \sigma_1 - \sigma_2$  (from bottom to top). The curves have been obtained by averaging on 20 000 time origins  $t_0$ . (b) Cooperativity number of the local shear stress at the borders, in comparison with the cooperativity number in the center of the sample

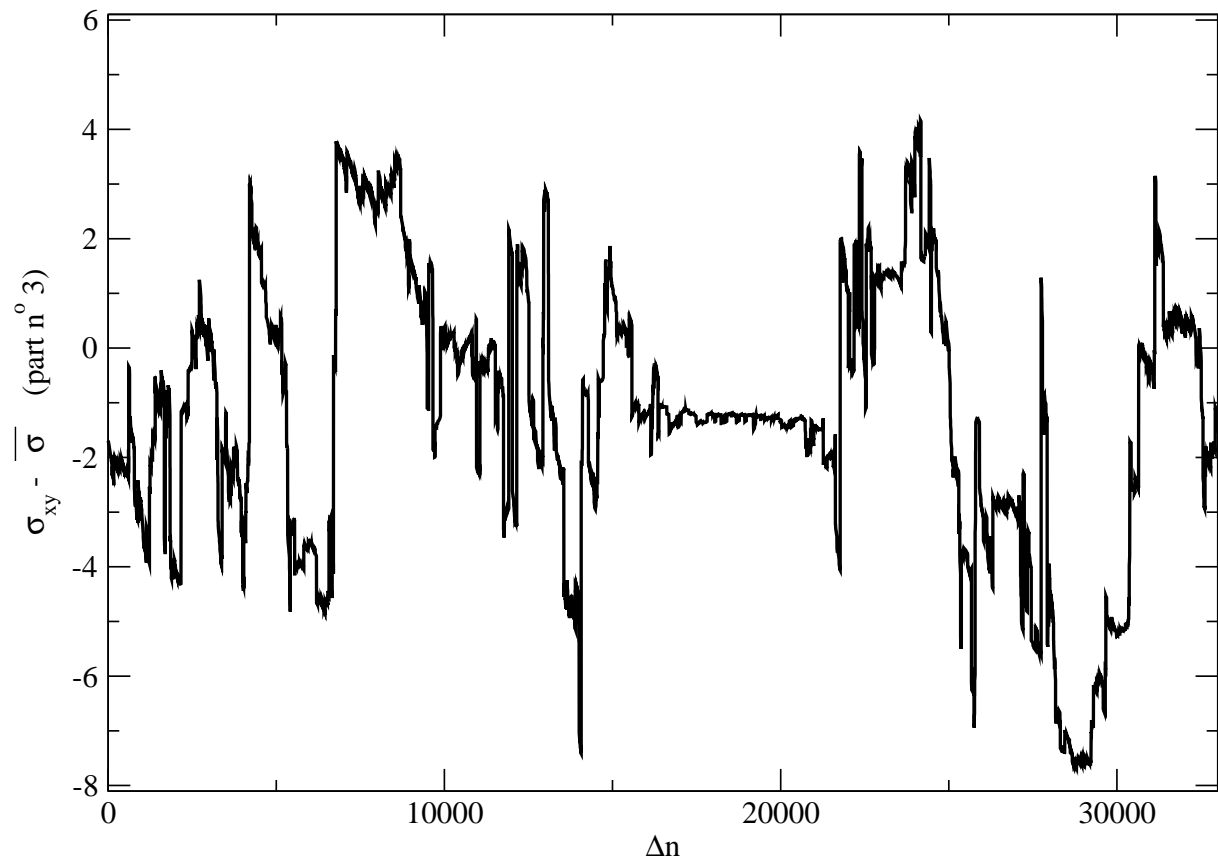


**Fig. 5.** Evolution of the shear stress on a given particle in the center of the sample, as a function of the applied shear strain. For each value, the average over the sample has been subtracted.

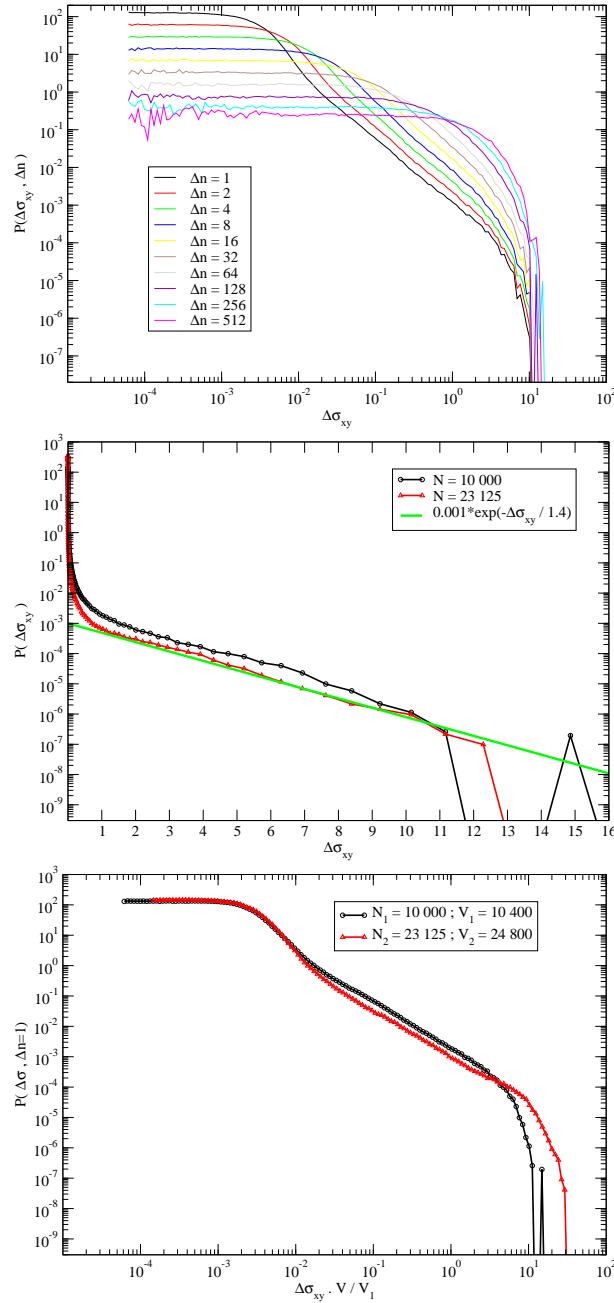


**Fig. 6.** (a) distribution  $P(\Delta\sigma_{xy}, \Delta n)$  of the variation of local shear stress  $\Delta\sigma_{xy}$  for different strain intervals  $\Delta n$ . The distribution has been obtained by averaging over the whole sample, and for different time origins. (b) lin-log scale for  $P(\Delta\sigma_{xy}, \Delta n = 1)$  and different system sizes  $N = 10000(104 \times 104)$  and  $N = 23125(50 \times 500)$ . It shows a size independent exponential upper cut-off with a characteristic  $\Delta\sigma \approx 1.4$ . (c) log-log scale for  $P(\Delta\sigma_{xy}, \Delta n = 1)$  and different system sizes  $N = 10000(104 \times 104)$  and  $N = 23125(50 \times 500)$ . It shows the scaling of the first cross-over  $\propto 1/V$  where  $V$  is the volume of the system. The stress variation is mainly due to local variation that averages over the whole system (see text).

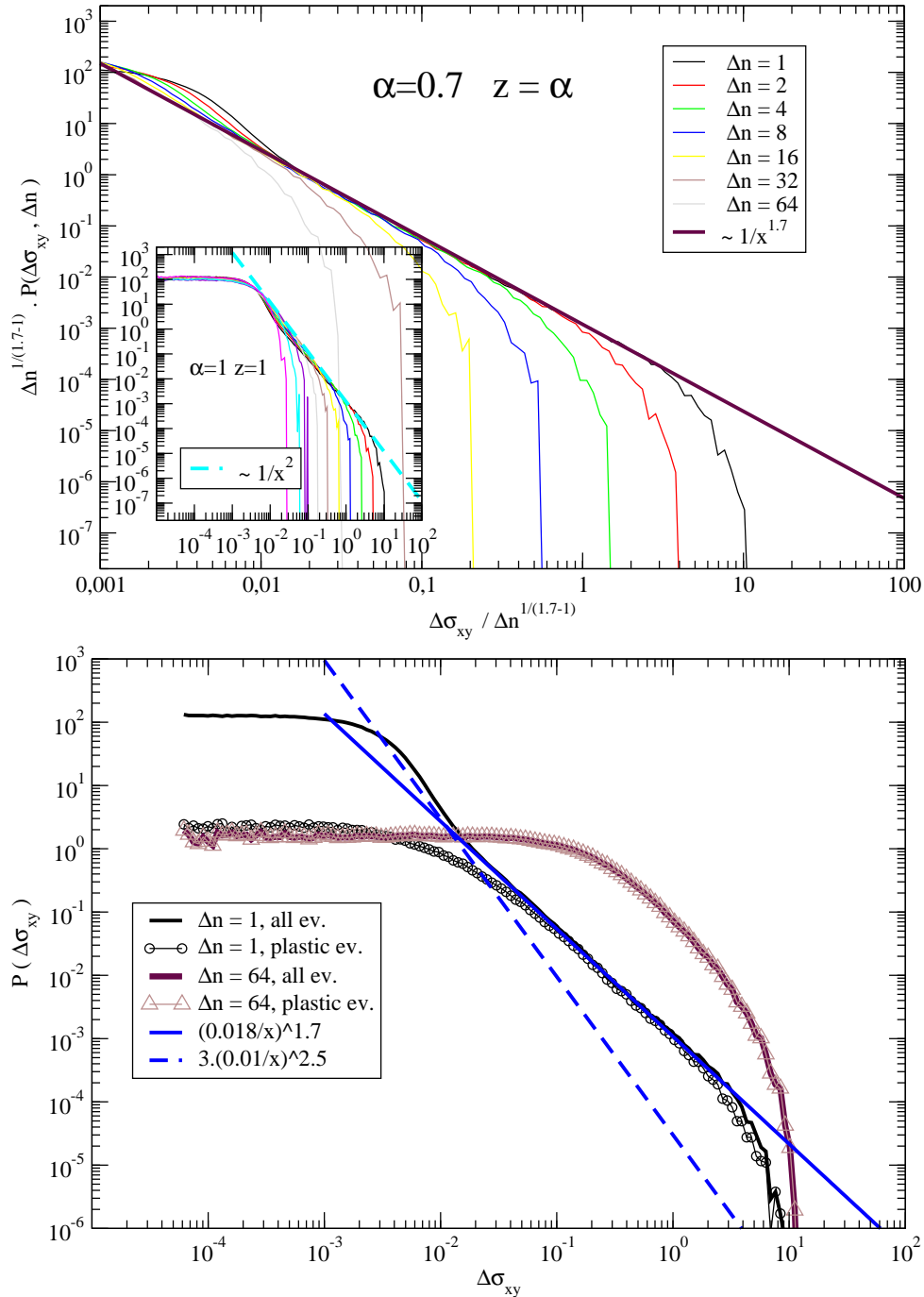


**Fig. 7.** (a) scaling of  $P(\Delta\sigma_{xy}, \Delta n) \propto \phi(\Delta\sigma_{xy}/\Delta n^{1/z})$  with  $z = \alpha$  and  $\alpha = 0.7$ . The scaling is very good in the intermediate range of the distribution, and for small  $\Delta n < 64$  where the exponential cut-off does not play a role. Inset: the same with  $\alpha = 1 = z$ . This exponent corresponds also to the one discussed in the text. (b) separate contribution of steps associated with a release of stress at a macroscopic level, to the total distribution of local stresses, for time intervals  $\Delta n = 1$  and  $\Delta n = 64$

. As shown here, the distribution of  $\Delta\sigma$  for  $\Delta n \geq 64$  is dominated by the contribution of stress changes due to plastic events.

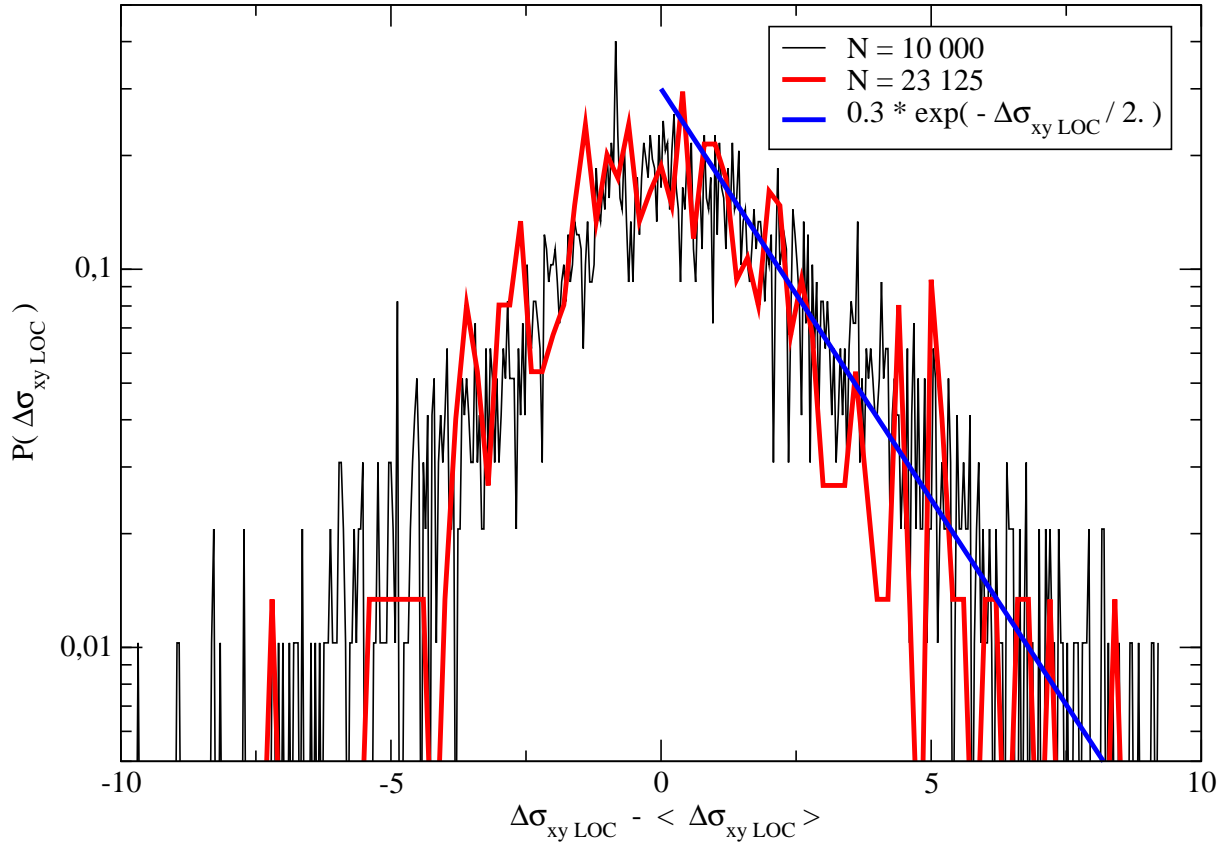


**Fig. 8.** Distribution of shear stress releases in the center of the quadrupoles, during a plastic event. The fit is exponential with a characteristic  $\Delta\sigma = 2$ .

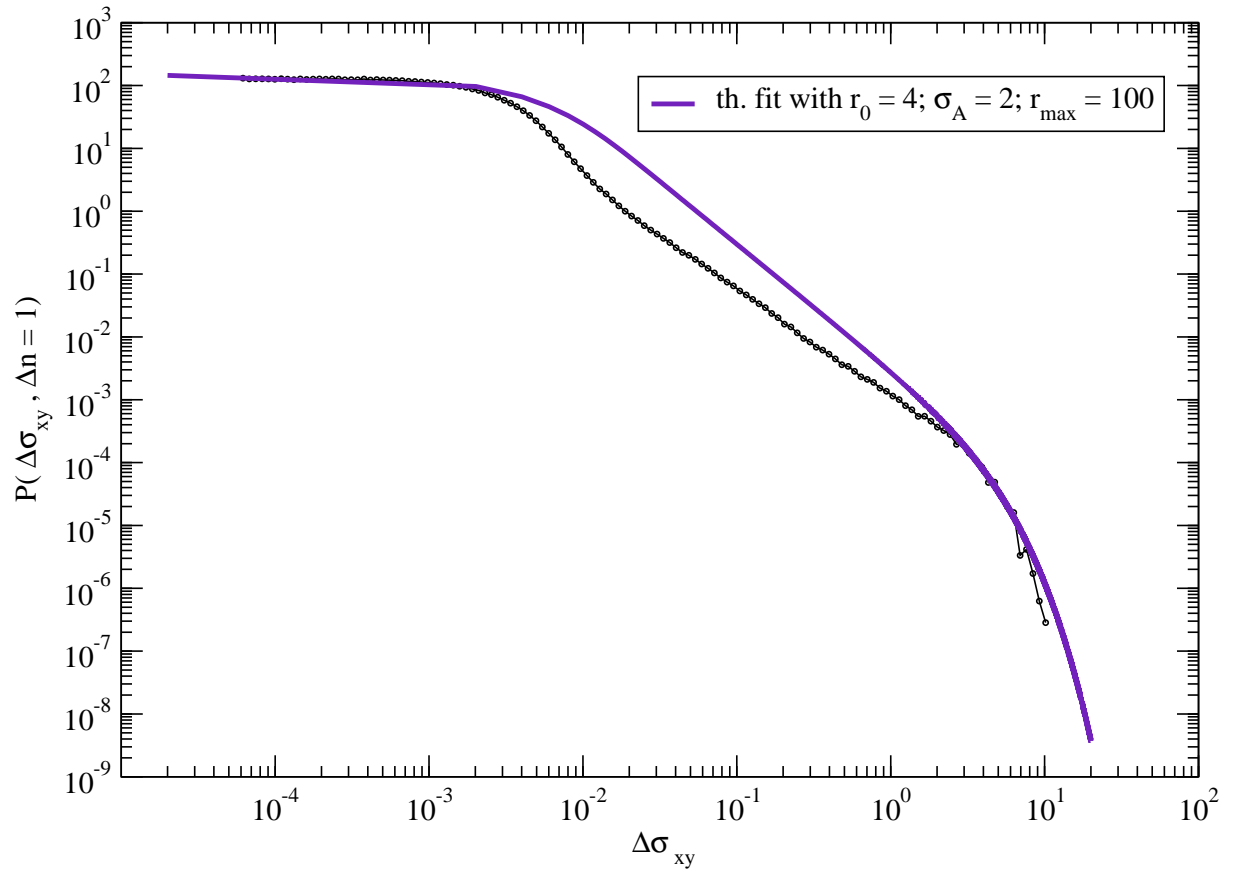


**Fig. 9.** Comparison of the distribution  $P(\Delta\sigma_{xy}, \Delta n = 1)$  with the theoretical fit discussed in the text. The parameters of the fit are indicated in the legend box.

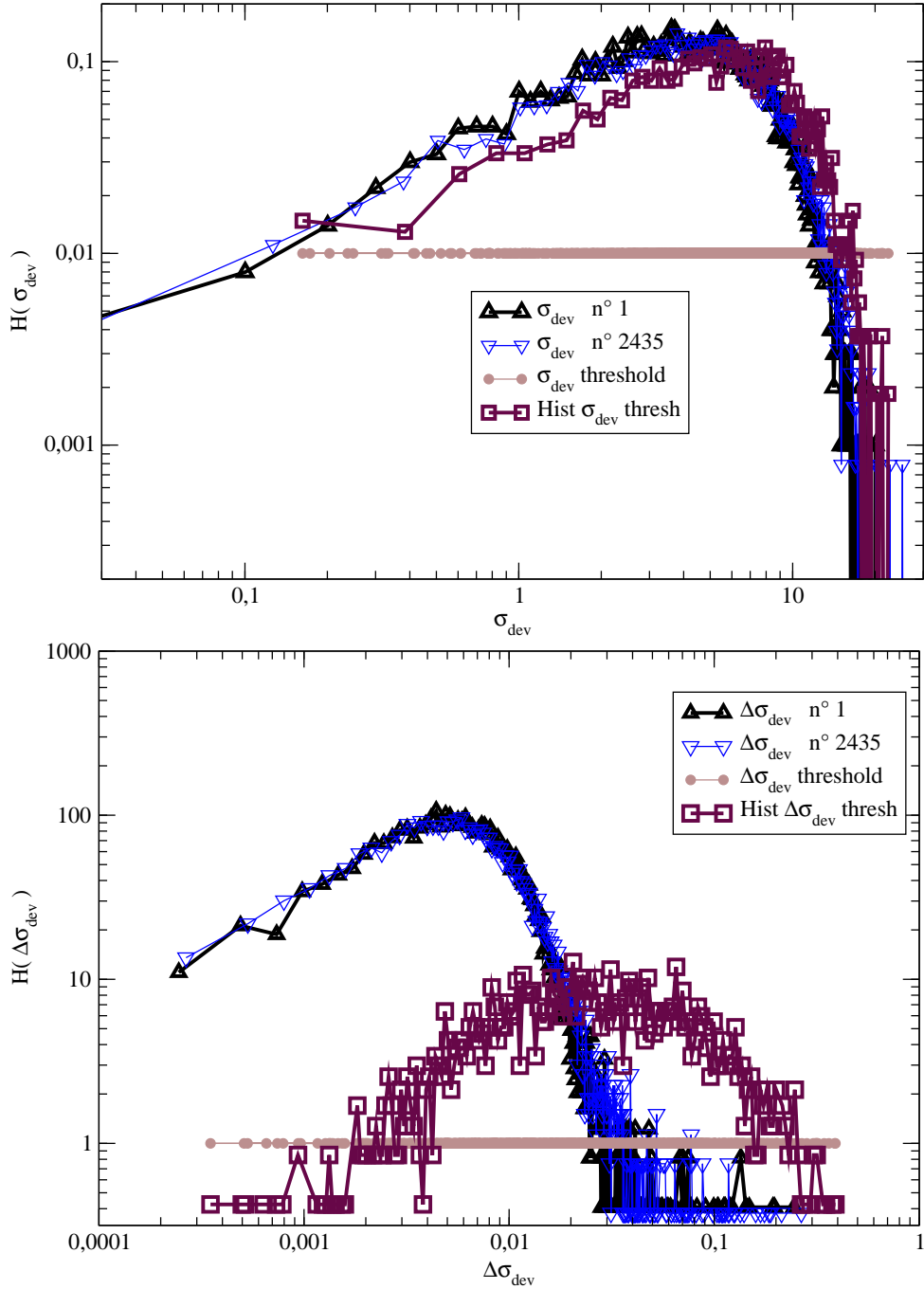


**Fig. 10.** (a) Distribution of the deviatoric stress in a configuration of 10 000 particles for 2 different strains in the beginning and in the end of the plastic flow plateau (triangles). Comparison with the distribution of the deviatoric stress in the center of the future quadrupole just before the quadrupolar event takes place (squares), computed on the 2500 plastic events of the plastic flow regime. The 3 curves are very similar. (b) Same as in (a), but for the *incremental* deviatoric stress. In this case, the distribution obtained on the center of the quadrupoles indicates a more pronounced correspondance with the highest incremental stresses inside the sample.